Applications and Applied Mathematics: An International Journal (AAM)

Volume 10 | Issue 2 Article 30

12-2015

Seir Model of Seasonal Epidemic Diseases using HAM

Nirmala P. Ratchagar
Annamalai University

S. P. Subramanian
Annamalai University

Available at
http://pvamu.edu/aam
Appl. Appl. Math.
ISSN: 1932-9466

Vol. 10, Issue 2 (December 2015), pp. 1066-1081

Applications and Applied Mathematics:
An International Journal
(AAM)

Seir Model of Seasonal Epidemic Diseases using HAM

Nirmala P. Ratchagar
Department of Mathematics
Annamalai University
Tamil Nadu, India

S. P. Subramanian
Mathematics Section
FEAT, Annamalai University
Tamil Nadu, India
aucse_n@yahoo.com

Received: March 11, 2015; Accepted: September 2, 2015

Abstract

SEIR mathematical model of childhood diseases measles, chickenpox, mumps, rubella incorporate seasonal variation in contact rates due to the increased mixing during school terms compared to school holidays. Driven by seasonality these diseases are characterized by annual oscillations with variable contact rate which is a periodic function of time in years. Homotopy Analysis Method (HAM) is considered in this paper to obtain a semi analytic approximate solution of non-linear simultaneous differential equations. Mathematica is used to carry out the computations. Results established through graphs show the validity and potential of HAM for amplitude of variation greater than zero. Also, when it is equal to zero both HAM and Runge-Kutta method graphs are compared.

Keywords: Latent class; Latent rate; Infection rate; Recovery rate; Variable Contact rate; Basic reproduction number

MSC (2010): 97M60

1. Introduction

In recent years, our understanding of infectious disease epidemiology and control has greatly increased through mathematical modeling. The first mathematical model about smallpox was formulated and solved (Bernoulli, 1760). The second Nobel Prize in medicine was won by Ross, for his mathematical (Differential equation) models for Malaria in 1911(Ross, 1911).

Diseases are unavoidable part of human life. We are very much afraid about the recently observed diseases such as Ebola, AIDS (HIV), Bird flu (Avian Influenza H5N1), Pig flu (Swine flu H1N1), Dengue fever, etc. In the fast moving world, a simple but powerful

technique is mathematical modeling which has been used to understand and predict the spread of the epidemic diseases. Designing the model, parameter estimation and interpretation are the vital parts of mathematical modeling. Understanding for mathematical modeling of epidemic diseases is very much useful for policy makers, researchers, public health and pharmaceutical professionals (Pei et al., 2014).

The key element in this field of research is being able to link mathematical model and simulation data. Both epidemiological data and findings of mathematical model studies can be compared for optimal result and guidance. Mathematical modeling plays a vital role in highest level of policy making in most of the exciting and increasingly important fields including health economic aspects, emergency planning, monitoring of surveillance data, risk assessment and control (Pei et al., 2014), an epidemic model in which age is taken into account (El-Doma, 2006; Li and Fang, 2009).

This model starts with the assumption that the total population N is constant at any time 't' and the individuals are homogeneous and mix uniformly. Also the basic assumption is that the population can be subdivided into four sets of distinct classes depending upon their experience with respect to disease. The model classifies individual as susceptible, exposed, infectious, recovered and hence it is also called SEIR mathematical model. Individual are born into the susceptible class $S(t)$. Susceptible individuals who have never come into contact with the disease and are able to catch the disease, but not able to spread are said to be in exposed class $E(t)$. Exposed individuals remain in the same class up to the latent period ($1/\varepsilon$). When the exposed individuals start to spread the disease they are said to move into the infectious class $I(t)$. Infected individuals spread the disease to susceptible and remain in the infectious class for a given period of time (the infectious period $=1/\gamma$) before moving into the recovered class. Finally the individuals in the recovered class are assumed to be immune for life. Hence, the total population $= N = S(t) + E(t) + I(t) + R(t)$.

The definition of contact rate without seasonality is $\beta = R_0(\gamma+\varepsilon+d)/N$. The modified definition of variable contact rate with seasonality $\beta = \beta(t)$ is explained. If a fundamental parameter governs the spread of a disease then, R_0 is defined by epidemiologists as "The average number of secondary cases caused by an infectious individual in a totally susceptible population". When $R_0 > 1$, the diseases can enter a totally susceptible population and the number of infected cases will increase, whereas when $R_0 \leq 1$, the diseases will always fail to spread.

Transmission of infectious diseases often depends on seasonal variability. Mathematical epidemic models driven by seasonal forcing have been widely explored to understand recurrent outbreaks of infectious diseases. Here we present an effective Homotopy Analysis Method (HAM) to examine the impact of seasonal variation patterns on epidemic dynamics. Seasonal change in the incidence of infectious disease is a common phenomenon of both temperature and tropical climates. Seasonal cycles of infectious diseases are universal and no single theory has provided satisfactory explanations about their cause. More than one explanation or combination of explanations may be true.

We observe the numerical solutions and graphs obtained by Adam decomposition method (Batiha, 2011), Variational iteration method (Biazar, 2006), Homotopy perturbation method

(Rafei et al., 2007a), and Differential transform method (Rafei et al., 2007b). These methods are valid only for small value of time. We divide the range into sub intervals and use HAM to

each of these intervals, which agree well with the numerical results already obtained for the same problem.

A crude approximation of the seasonality is to assume sinusoidality:

$$\beta(t) = \beta_0 (1+\alpha \cos(2\pi t))$$

$$\beta(t) = \begin{cases} 0, (\text{minimum}), & \text{during holidays,} \\ 2\beta_0, (\text{maximum}), & \text{during school days .} \end{cases}$$

Here 'β_0' is mean contact rate, 'α' is the amplitude of seasonal variation ($0 \leq \alpha \leq 1$) and 't' is assumed to be measured in years. $\beta(t)$ is assumed to be periodic function (with period 1 year) (Greenhalgh, 2014).

The differential equations of seasonally forced SEIR model are

$$\frac{dS}{dt} = -\beta(t)SI \tag{1}$$

$$\frac{dE}{dt} = \beta(t)SI - \varepsilon E \tag{2}$$

$$\frac{dI}{dt} = \varepsilon E - \gamma I \tag{3}$$

$$\frac{dR}{dt} = \gamma I \tag{4}$$

where, $\varepsilon, \gamma > 0$ and with initial conditions

$S(0) = Ns$, $E(0) = N_E$, $I(0) = N_I$, $R(0) = N_R$.

Particularly, we have considered four cases for childhood diseases (i) Measles, (ii) Chickenpox, (iii) Mumps and (iv) Rubella.

2. Basic idea of HAM

Consider $N[U(t)] = 0$, where, N is any operator, $U(t)$ is unknown function, 't' the independent variable, $U_0(t)$ is initial guess of the exact solution, $U(t)$, $h \neq 0$ is an auxiliary parameter, $H(t) \neq 0$ is auxiliary function, and L is an auxiliary linear operator with the property that $L[U(t)] = 0$ when $U(t) = 0$. Then, using $p \in [0, 1]$ as an embedding parameter, we construct a homotopy

$$(1-p)L[f(t;p) - U_0(t)] - phH(t)\, N[f(t;p)] = \widehat{H}. \tag{5}$$

We can choose the initial guess $U_0(t)$, the auxiliary linear operator L, the nonzero auxiliary parameter 'h' and the auxiliary function $H(t)$ suitably. Equating the homotopy (5) to zero, we get the zero order deformation equation.

$$(1-p)L[f(t;p)-U_0(t)]=phH(t)\,N[f(t;p)] \tag{6}$$

When $p = 0$, the zero order deformation Equation (6) becomes

$$L[f(t;0)-U_0(t)]=0$$

$$f(t;0)-U_0(t),\ initial\ \ approximation \tag{7}$$

and when $p = 1$, since $h \neq 0$ and $H(t) \neq 0$, the zero-order deformation Equation (6) is equivalent to $N[f(t;1)] = 0$. Therefore,

$$f(t;1)–U(t),\ exact\ solution \tag{8}$$

As the embedding parameter 'p' increases from '0' to '1', $f(t;p)$ varies continuously from the initial approximation $U_0(t)$ to the exact solution $U(t)$. Such kind of continuous variation is called deformation in homotopy. $f(t;p)$ can be expanded using Taylor's Theorem

$$f(t;p) = U_0(t) + \sum_{m=1}^{\infty} U_m(t)p^m, \tag{9}$$

where,

$$U_m(t) = \frac{1}{m!}\frac{\partial^m f(t;p)}{\partial p^m}\Big|_{p=0}. \tag{10}$$

If the initial guess $U_0(t)$, the auxiliary linear operator L, the non-zero auxiliary parameter 'h' and the auxiliary function $H(t)$ are properly chosen, then

i) the solution $f(t; p)$ of the zero order deformation Equation (6) exists for all $p \in [0,1]$,

ii) $\frac{\partial^m f(t;p)}{\partial p^m}\Big|_{p=0}$ exists for $m = 1,2,3,\ldots$, and

iii) the power series (9) of $f(t;p)$ converges at $p = 1$.

Under these assumptions the solution series, reduces to

$$f(t;1) = U_0(t) + \sum_{m=1}^{\infty} U_m(t)\,. \tag{11}$$

We define the vector

$$\overrightarrow{U_n}(t) = \{U_0(t), U_1(t), U_2(t), \ldots, U_n(t)\}\quad . \tag{12}$$

According to definition (10), $U_m(t)$ can be derived from the zero-order deformation Equation (6). Differentiating the zero-order deformation equation 'm' times with respect to 'p' and then dividing by '$m!$' and finally setting p=0, we have the so called m^{th} order deformation equation.

$$L[U_m(t) - \alpha_m U_{m-1}(t)] = h H(t) R_m(U_{m-1}(t)), \quad (13)$$

where

$$R_m(U_{m-1}(t)) = \frac{1}{(m-1)!}\frac{\partial^{m-1} N[f(t;p)]}{\partial p^{m-1}} \quad (14)$$

and

$$\alpha_m = \begin{cases} 0, & m \leq 1, \\ 1, & m > 1. \end{cases}$$

The higher order deformation Equation (13) is governed by the linear operator L, and the term $R_m(U_{m-1}(t))$ can be expressed simply by (14) for any non-linear operator N.

According to definition (14), the right-hand side of Equation (13) is only dependent upon $U_{m-1}(t)$. Thus, we get $U_1(t)$, $U_2(t)$,..., by means of solving the linear higher order deformation Equation (13) one after the other in order.

3. Solution of the SEIR model by HAM

The system described by Equations (1) - (4) can be solved using non perturbation method HAM with the help of Equations (7) and (8). The advantage of this method is that it provides a direct scheme for solving the problem.

To apply the HAM, we choose

$$S_0(t)=N_s\ ,\ E_0(t)=N_E,\ I_0(t)=N_I,\ R_0(t)=N_R$$

as initial approximations of $S(t)$, $E(t)$, $I(t)$, $R(t)$ respectively. Let $p \in [0,1]$ be the so called embedding parameter; then HAM is based on a kind of continuous mappings

$$S(t) \to f_1(t;p),\ E(t) \to f_2(t;p),\ I(t) \to f_3(t;p),\ R(t) \to f_4(t;p),$$

such that, as the embedding parameter 'p' increases from '0' to '1', $f_i(t;p)$ varies from the initial approximation to the exact solution. To ensure this, choose such auxiliary linear operators as

$L[f_i(t;p)] = \frac{\partial f_i(t;p)}{\partial t},\ i = 1, 2, 3\ 4,$

with the property

$L_i(C_i)=0$, where C_i are integral constants.

The nonlinear operators are

$$N_1[f_i(t;p)] = \frac{\partial f_i(t;p)}{\partial t} + \beta(t) f_i(t;p) f_3(t;p),$$

$$N_2[f_i(t;p)] = \frac{\partial f_i(t;p)}{\partial t} - \beta(t) f_1(t;p) f_3(t;p) + \varepsilon f_i(t;p),$$

$$N_3[f_i(t;p)] = \frac{\partial f_i(t;p)}{\partial t} - \varepsilon f_2(t;p) + \gamma f_i(t;p),$$

$$N_4[f_i(t;p)] = \frac{\partial f_i(t;p)}{\partial t} - \gamma f_3(t;p).$$

Let $h_i \neq 0$ and $H_i(t) \neq 0$ denote the so called auxiliary parameter and auxiliary function, respectively. Using the embedding parameter p we construct a family of equations,

$(1\text{-}p)\ L\ [f_1(t;p)\text{-}S_0(t)] = p h_1 H_1(t) N_1[f_1(t;p)]$,

$(1\text{-}p)\ L\ [f_2(t;p)\text{-}E_0(t)] = p h_2 H_2(t) N_2[f_2(t;p)]$,

$(1\text{-}p)\ L\ [f_3(t;p)\text{-}I_0(t)] = p h_3 H_3(t) N_3[f_3(t;p)]$,

$(1\text{-}p)\ L\ [f_4(t;p)\text{-}R_0(t)] = p h_4 H_4(t) N_4[f_4(t;p)]$,

subject to the initial conditions

$f_1(0;p) = S_0,\ f_2(0;p) = E_0,\ f_3(0;p) = I_0,\ f_4(0;p) = R_0.$

Using Taylor's Theorem, we expand $f_i(t;p)$ by a power series of the embedding parameter p as follows:

$$f_1(t;p) = S_0(t) + \sum_{m=1}^{\infty} S_m(t) p^m,$$

$$f_2(t;p) = E_0(t) + \sum_{m=1}^{\infty} E_m(t) p^m,$$

$$f_3(t;p) = I_0(t) + \sum_{m=1}^{\infty} I_m(t) p^m,$$

$$f_4(t;p) = R_0(t) + \sum_{m=1}^{\infty} R_m(t) p^m,$$

where

$$S_m(t) = \frac{1}{m!}\frac{\partial^m f_1(t;p)}{\partial p^m}\Big|_{p=0},$$

$$E_m(t) = \frac{1}{m!}\frac{\partial^m f_2(t;p)}{\partial p^m}\Big|_{p=0},$$

$$I_m(t) = \frac{1}{m!}\frac{\partial^m f_3(t;p)}{\partial p^m}\Big|_{p=0},$$

$$R_m(t) = \frac{1}{m!}\frac{\partial^m f_4(t;p)}{\partial p^m}\Big|_{p=0}.$$

From the so-called m^{th} order deformation Equations (13) and (14), we have

$$\begin{aligned} &L[S_m(t) - \alpha_m S_{m-1}(t)] = h_1 H_1(t) R_m(S_{m-1}(t)), \\ &L[E_m(t) - \alpha_m E_{m-1}(t)] = h_2 H_2(t) R_m(E_{m-1}(t)), \\ &L[I_m(t) - \alpha_m I_{m-1}(t)] = h_3 H_3(t) R_m(I_{m-1}(t)), \\ &L[R_m(t) - \alpha_m R_{m-1}(t)] = h_4 H_4(t) R_m(R_{m-1}(t)), \\ &S_m(0) = 0,\ E_m(0) = 0,\ I_m(0) = 0,\ R_m(0) = 0. \end{aligned} \quad (15)$$

We use "*h*-curves" suggested by the author (Liao, 1998, 2003, 2004). It is reasonable to use *hi* = -1 and $H_i(t)$=1 the m^{th} order deformation equation (15) for $m \geq 1$ becomes.

$$S_m(t) = \alpha_m S_{m-1}(t) - \int_0^t [S'_{m-1}(t) + \beta(t) \sum_{k=0}^{m-1} S_k(t) I_{m-1-k}(t)]\, dt, \quad (16)$$

$$E_m(t) = \alpha_m E_{m-1}(t) - \int_0^t [E'_{m-1}(t) - \beta(t) \sum_{k=0}^{m-1} S_k(t) I_{m-1-k}(t) + \varepsilon E_{m-1}(t)]\, dt, \quad (17)$$

$$I_m(t) = \alpha_m I_{m-1}(t) - \int_0^t [I'_{m-1}(t) - \varepsilon E_{m-1}(t) + \gamma I_{m-1}(t)]\, dt, \quad (18)$$

$$R_m(t) = \alpha_m R_{m-1}(t) - \int_0^t [R'_{m-1}(t) - \gamma I_{m-1}(t)]\, dt. \quad (19)$$

4. Numerical Calculation

For numerical results, we consider

S [0] = 10,00,000, *E*[0] =100, *I* [0] =100, *R*[0]=0 (Moneim, 2006).

Table 1. Recovery (infectious) rate (γ), latent rate(ε) and mean contact rate (β_0)

	ε **(in year)**	γ **(in year)**	β_0 **(per year)**
Measles	(365/9.49)	(365/3.65)	0.0018
Chicken Pox	(365/15.22)	(365/9.13)	0.00113
Mumps	(365/18.26)	(365/11.17)	0.00081
Rubella (3 days Measles)	(365/110.65)	(365/11.67)	0.0007

We use a new approach by dividing the domain $0 \leq t \leq L$ into subintervals with different lengths. Each subinterval represent H_i , such that $\sum H_i=L$, i=1, 2, 3,…. We apply direct scheme (16), (17), (18), (19) and $S(t)=\sum_{m=0}^{4} S(m)$, $E(t)=\sum_{m=0}^{4} E(m)$, $I(t)=\sum_{m=0}^{4} I(m)$, $R(t)=\sum_{m=0}^{4} R(m)$ of HAM in each of these subintervals, one after another in order. By taking time *'t'* in years we study the problem for four childhood diseases.

We have also used fourth and fifth order Runge-Kutta method along with variable step size method when α=0 (epidemic diseases without seasonality) for all the four childhood diseases Runge-Kutta method cannot be used when α=0. The results for both HAM and Runge-Kutta method have been compared and discussed through graphs.

5. Result and Discussion

Figures 1 and 2 show seasonal variation of population effected by measles when the amplitude of seasonal variation α=0 using HAM and Runge-Kutta method respectively. It is observed that while using HAM the curves in the figures are non-smooth, but when Runge-Kutta method was applied it was possible to get smooth curves as shown in Figure 2.

When α=0.5 and α=1, we were able to apply only HAM as shown in Figures 3 and 4. Since the equations become transcendental equations, it is not possible to obtain numerical results by Runge-Kutta method. Hence the curves in Figures 3 and 4 are not very smooth.

From Figures 1and 2, we see that susceptible population gradually decreases from 10,00,000, both infected and exposed population increase from 100, the recovered population increase from zero. There are four critical points of susceptible population, one with exposed population 4,05,458 at time *t* (in years) = 0.059800325 (HAM), also with exposed population 4,40,616 at time *t* (in years) = 0.0391589465731220 (Runge-Kutta method); second with infected population 1,54,835 at time *t* (in years) = 0.06766226 (HAM), also with infected population 1,27,990 at time *t* (in years) = 0.0456296873558348 (Runge-Kutta method); third with recovered population 1,85,228 at time t (in years) =0.066595803 (HAM), also with recovered population 1,18,509 at time t(in years) = 0.0458960396513443 (Runge-Kutta method). The fourth critical point occurs between infected population 1,20,811 with recovered population at time *t* (in years) =0.0627375 (HAM), also infected population 1,69,767 with recovered population at time *t* (in years) = 0.0491552563529539 (Runge-Kutta method).The exposed population increases from 100 will have a fifth critical point with recovered population 4,07,833 at time *t*=0.0618958836623334 (Runge-Kutta method).

Figure 3 depicts that exposed population increase from 100 and attain the peak when the exposed population is 7,56,622.5 at time t = 0.048. Here one critical point occurs between susceptible population 4,47,487 with exposed population at time t = 0.04386525. The second critical point occurs when the susceptible population curve meets the infected population

curve with the same population 1,01,608 at time t = 0.04767402. There are two more critical points; one between susceptible and recovered population 72,150.2 at time t = 0.04794239, and, second between infected and recovered population 1,87,951 at time t = 0.0554698 (HAM).

Figure 4 indicates that, there are six critical points as explained below and one peak point of exposed population 7,40,532.5 at time t = 0.038. The critical points of susceptible population are one with exposed population 4,67,151 at time t = 0.03624357, second with infected population 1,05,520 at time t = 0.04119053, third with recovered population 77,759.6 at time t = 0.04248692. The fourth and fifth critical points occur between infected and recovered populations 1,92,736 and 38,803.6 at time t = 0.0493539 and t = 0.03785488 respectively. The sixth critical point is between exposed and infected population 27,071.1 at time t=0.0297934 (HAM).

Figures 5 and 6 show seasonal variation of population effected by chickenpox when the amplitude of seasonal variation α = 0 using HAM and Runge-Kutta method respectively. HAM curves are non-smooth and Runge-Kutta method curves are smooth. Runge-Kutta method cannot be applied, for α = 0.5 and 1, since the equations become transcendental equations. Using HAM non-smooth curves are obtained as shown in Figures 7 and 8.

Figures 5 and 6 reveal that there are four critical points of susceptible population, one exposed population 4,32,899 at time t = 0.0666156 (HAM), also exposed population 4,45,763 at time t = 0.0573016050041030 (Runge-Kutta method); second with infected population 1,59,794 at time t = 0.07398059 (HAM), also with infected population 1,50,070 at time t=0.0656095917124844 (Runge-Kutta method); third with recovered population 1,00,845 at time t = 0.078247555 (HAM), also with recovered population 86,842 at t = 0.0687700475434419(Runge-Kutta method); fourth critical point between infected and recovered population 2,63,486 at time t = 0.0953938 (HAM), also infected and recovered population 2,62,797 at time t = 0.0875855498588225 (Runge-Kutta method).The exposed population will increase from 100 and intersect with $R(t)$ = 3,71,594 at t = 0.0976955859641300 (Runge-Kutta method).

It is observed from Figure 7 that the exposed population increased from 100 and gradually it attains the peak population 7,89,547.5 at time t = 0.064 (HAM). Susceptible population curve meets the other three curves, first with exposed population curve when the population 4,46,413 at time t = 0.059025701, second with infected population curve with population 1,21,786 at time t = 0.06315313, third with recovered population 41,545.6 at time t = 0.064000495 (HAM).

Three critical points are observed from Figure 8; first, between susceptible and exposed population 4,32,457 at time t = 0.05326775, second between susceptible and infected population 2,43,779 at time t = 0.05836153, third between exposed and infected population 4,43,071 at time t = 0.063746626.

Figures 9 and 10 show seasonal variation of population effected by mumps when the amplitude of seasonal variation α = 0 using HAM and Runge-Kutta method respectively. It is observed that while using HAM, the curves in the figures are non-smooth, but when Runge-Kutta method was applied it was possible to get smooth curves as shown in Figure 10.

It is seen from Figures 9 and 10 that the susceptible population gradually decrease from 10,00,000 over time and met with all the other three population curves, with exposed population 4,30,359 at t time t = 0.07328232 (HAM), also with exposed population 4,41,918 at t=0.0750913374988352(Runge-Kutta method); with infected population 1,62,151 at time t=0.09082556 (HAM), also with infected population 1,53,029 at t = 0.0860368235934791 (Runge-Kutta method); with recovered population 8,35,84.1 at time t = 0.084712159 (HAM), also with recovered population 95,339 at t = 0.0903366517691713 (Runge-Kutta method). The exposed population gradually increased from 100 and attains the peak population 643826 at time t = 0.00725 (HAM). The fourth critical point between infected and recovered population 2,71,049 at time t = 0.1083131 (HAM), also infected and recovered population 2,62,568 at t = 0.112220943783087 (Runge-Kutta method).

The exposed population increases from 100 and intersects with $R(t)$=3,70,930 at t=0.124447917943134 (Runge-Kutta method).

When α = 0.5 and α =1, we were able to apply only HAM as shown in Figures 11 and 12. Since the equations become transcendental equations it is not possible to obtain numerical results by Runge-Kutta method , hence the curves in Figures 11 and 12 are not very smooth.

Figure 11 depicts that exposed population attains the peak with the population 7,46,938 at time t = 0.074. Also, there are three critical points of susceptible population; first, with exposed population 4,28,316 at time t =0.068359882, second with infected population 1,54,169 at time t=0.07220432, third with recovered population 42,623.35 at time t=0.074324301.

Susceptible population of Figure 12 decreases from 10,00,000. The first critical point between susceptible and exposed population 4,61,775 at time t = 0.05817252, the second critical point between susceptible and infected population 1,53,089.5 at time t=0.0636215, the third critical point between susceptible and recovered population 16,716.05 at time t=0.06590506.

Figure 13 and 14 show seasonal variational of population effected by rubella when the amplitude of seasonal variation α = 0 using HAM and Runge-Kutta method respectively. HAM curves are non-smooth and Runge-Kutta method curves are smooth. Runge-Kutta method cannot be applied for α = 0.5 and 1, since the equations become transcendental equations. Using HAM non-smooth curves are obtained.

From Figures 13 and 14, we observe that there are five critical points. The susceptible population curve meets all the other three curves; first, critical point with exposed curve with population 4,11,644 at time t=0.059822825 (HAM), also with exposed curve with population 4,22,386 at t = 0.0649140762625283 (Runge-Kutta method); second critical point with infected population curve with the population 2,11,416 at time t = 0.06472393 (HAM), also with infected population curve with the population 1,82,309 at t = 0.0714320121485008 (Runge-Kutta method); third critical point with recovered population 81,989.6 at time t=0.06840353 (HAM), also with recovered population 1,02,189 at t = 0.0763903050507233 (Runge-Kutta method); The fourth and fifth critical points are between exposed and infected population 3,68,934.5 and 20,572 at time t = 0.0859048, and t = 0.04286284 respectively, (HAM).

$I(t)$ increases from 100 and intersects with recovered population 3,55,524 at t = 0.100906756640673. $E(t)$ increases from 100 and intersects with recovered population 3,21,062 at time t = 0.0977736354328306 (Runge-Kutta method).

Three critical points are seen in Figure 15. All the three critical points are with susceptible population, one with exposed population 4,40,930 at time t=0.05865708, second with infected population 2,03,839 at time t=0.062410962, third with recovered population 26,238.4 at time t = 0.065525961 (HAM).

From Figure 16, we observe that the exposed population starts from 100 and attains the peak population 7,84,910 at time t = 0.058. Three critical points of susceptible population are observed in this figure; first, with exposed population 4,63,724 at time t=0.053355815, second with infected population 1,40,867 at time t=0.05691012, and third with recovered population 19,577.9 at time t = 0.058291198 (HAM).

6. Conclusion

SEIR epidemic model with seasonal variation in the contact rate is analyzed. Four infectious diseases are studied (Measles, Chickenpox, Mumps and Rubella). The computer simulation results are obtained by taking sinusoidally varying contact rate. The results reveal that the proposed HAM is simple but very effective and highly successful in explaining the temporal dynamics of childhood diseases, by varying the amplitude (α = 0, 0.5 and 1). Since Runge-Kutta method cannot be applied when α = 0.5 and 1, from the available methods HAM is most suitable for SEIR model with seasonality. We have also shown that seasonality plays an important role for all these diseases.

REFERENCES

Batiha, A.M. and Batiha, B. (2011). A new method for solving epidemic model, Australian Journal of Basic and Applied Sciences,Vol. 5, No.12, 3122–3126.

Bernoulli, D.(1760). Essai d'une nouvelle analyse de la mortalite' cause'e par la petzte ve'role et des avantages de l'inoculation pour la pre'venir, in bICmoires de MathCmatiques et de Physique, AcadCmie Royale des Sciences, Paris,1-45.

Biazar, J. (2006). Solution of the epidemic model by Adomian decomposition method, Applied Mathematics and Computation, Vol. 173, No. 2, 1101–1106.

Earn, David J.D. (2004). Mathematical Modelling of Recurrent Epidemics, Math of Epidemic, 14-17.

E1-Doma, M. (2006). Analysis of SEIR Age structured epidemic model with vaccination and vertical transmission of disease, AAM, Vol. 1 No. 1, 36-61.

Greenhalgh, D. and Moneim, I. A. (2014). Periodicity in general seasonally driven epidemic models, Academicedu, 1-5.

Hethcote, H.W. (2000). The mathematics of infectious diseases, SIAM Review, Vol. 42, No. 4, 599–653.

Jordan, D. W. and Smith, P. (1999). Nonlinear Ordinary Differential Equations, Vol. 2, Oxford Texts in Applied and Engineering Mathematics, Oxford University Press, Oxford, UK, 3rd edition.

Liao,S.J. (1998). Homotopy analysis method: A new analytic method for nonlinear problems, Applied Mathematics and Mechanics, 957-962.

Liao, S.J. (2003). Beyond perturbation: introduction to the homotopy analysis method, Boca Raton: Chapman and Hall/CRC Press.

Liao, S.J. (2004). On the homotopy analysis method for nonlinear problems, Applied Mathematics and Computation, 499-513.

Li, X.Z. and Fang.B (2009). Stability of an Age structured SEIR Epidemic model with infectivity in latent period, AAM, Vol. 4, No. 1, 218-236.

Moneim, I.A. (2006). Seasonally varying epidemics with and without latent period: a comparative simulation study, Mathematics in Medicine and Biology, doi: 10.1093/ imammb/ dql023, 1-15.sss

Pei,Y., Li, C., Wu, Q., and Lv, Y. (2014). Successive Vaccination and Difference in Immunity of a Delay SIR Model with a General Incidence Rate. Abstract and Applied Analysis 2014, 1-10. Online publication date: 1-Jan-2014.

Rafei, M., Ganji, D. D.andAniali, H. (2007a). Solution of the epidemic model by Homotopyperturbation method, Applied Mathematics and Computation, Vol. 187, No. 2, 1056–1062.

Rafei, M., Daniali, H. and Ganji, D. D. (2007b).Variational iteration method for solving the epidemic model and the prey and predator problem, Applied Mathematics and Computation, Vol. 186, No. 2, 1701–1709.

Ross, R.(1911). The Prevention of Malaria.2nd edn. John Murry, London.

Tanaka, G. and Aihara, K. (2013). Effects of Seasonal Variation patterns on recurrent outbreaks in epidemic models, Journal of Theoretical Biology, Elsevier, 317, 87-95.

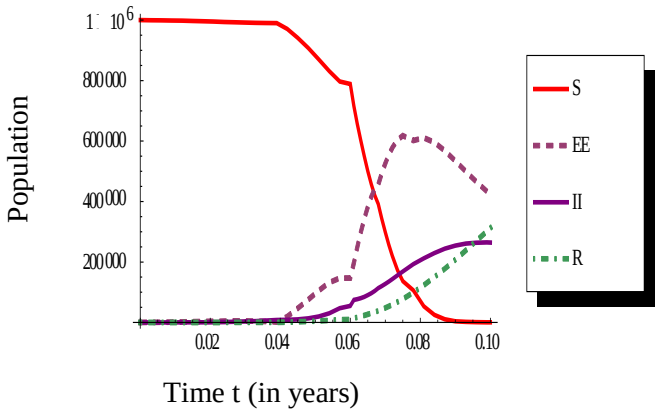

Figure 1. UsingHAM (α=0)

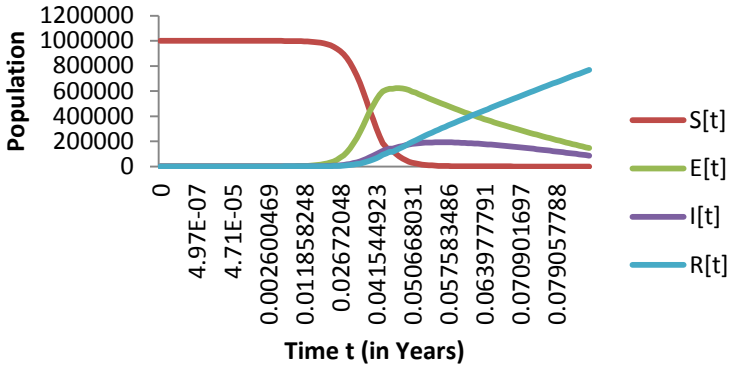

Figure 2. UsingRUNGE-KUTTA method (α=0)

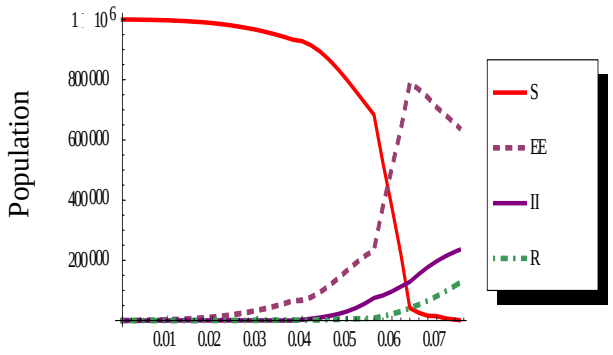

Figure 3. Using HAM (α=0.5)

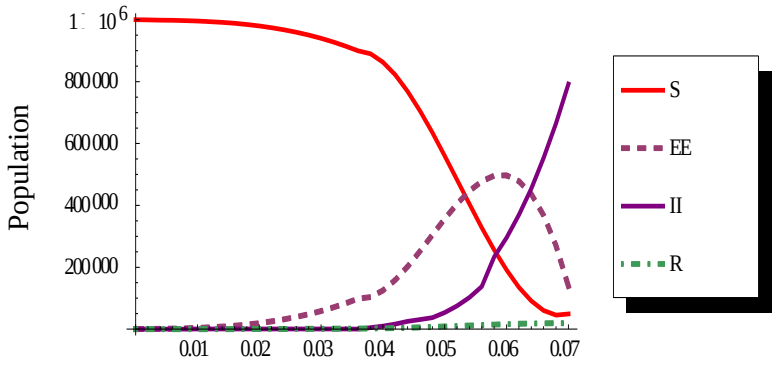

Figure 4. UsingHAM (α=1)

Variation of population with time for measles

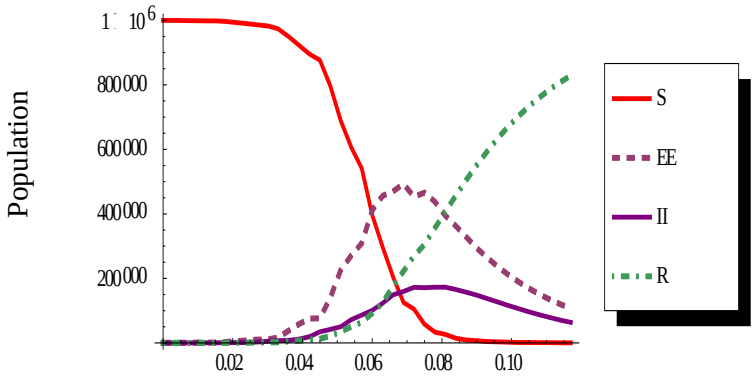

Time t (in years)

Figure 5.UsingHAM (α=0)

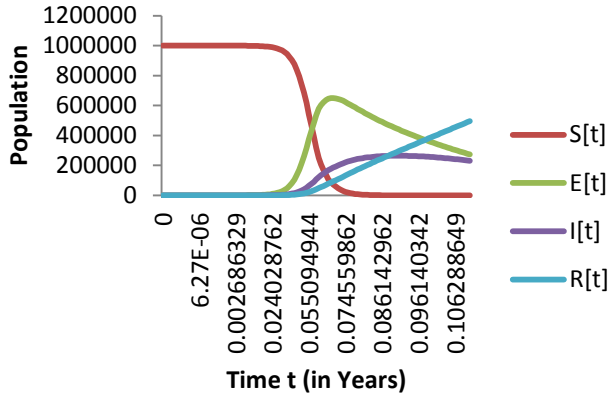

Figure 6.Using RUNGE-KUTTA method (α=0)

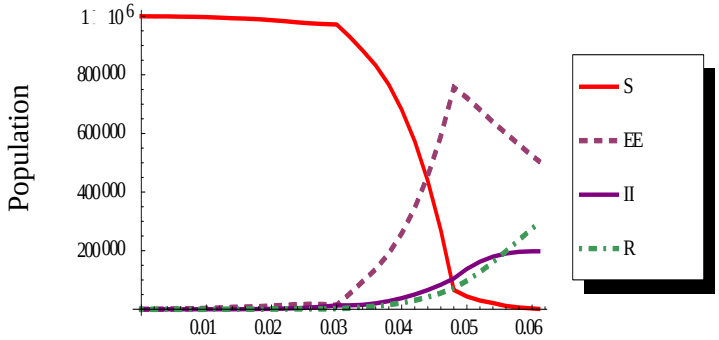

Time t (in years)

Figure 7.UsingHAM (α=0.5)

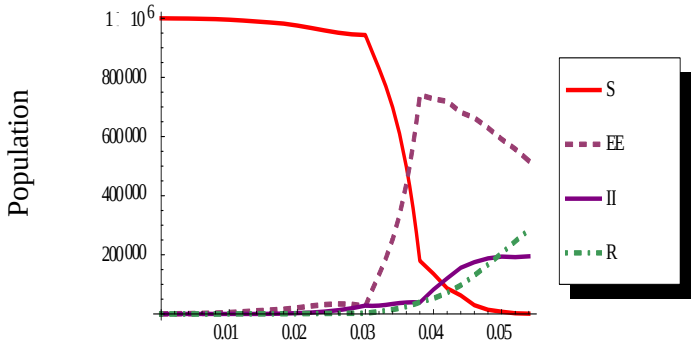

Time t (in years)

Figure 8.Using HAM (α=1)

Variation of population with time for chickenpox

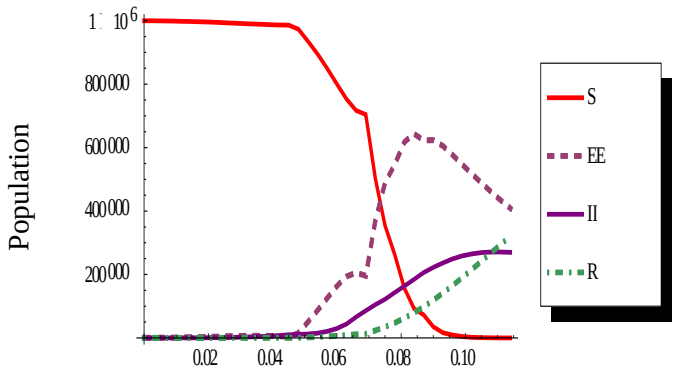

Time t (in years)

Figure 9.UsingHAM (α=0)

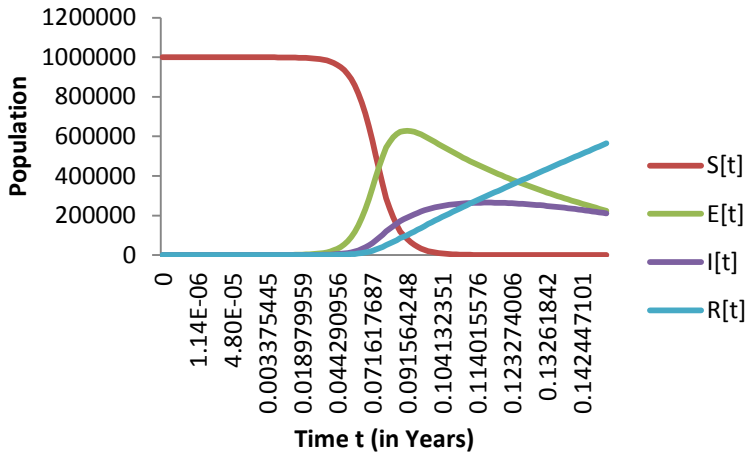

Figure 10.Using RUNGE-KUTTA method (α=0)

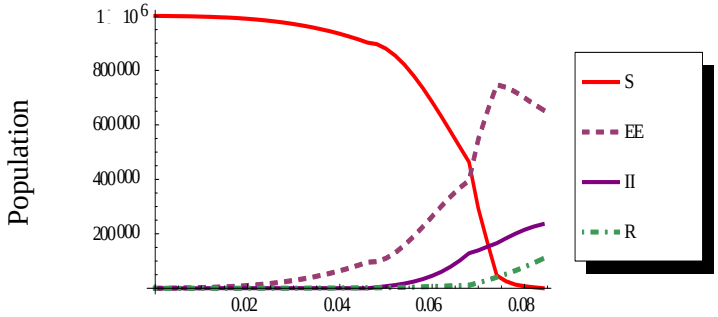

Time t (in years)

Figure 11.Using HAM (α=0.5)

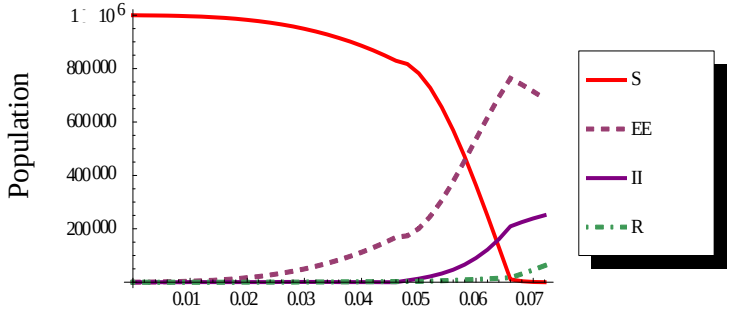

Time t (in years)

Figure 12.Using HAM (α=1)

Variation of population with time for mumps

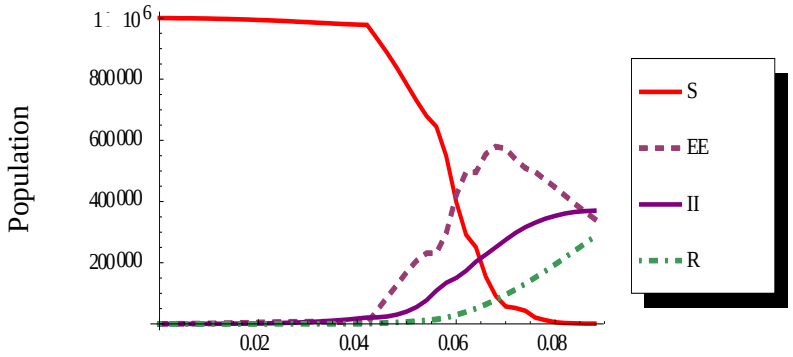

Time t (in years)

Figure 13.UsingHAM (α=0)

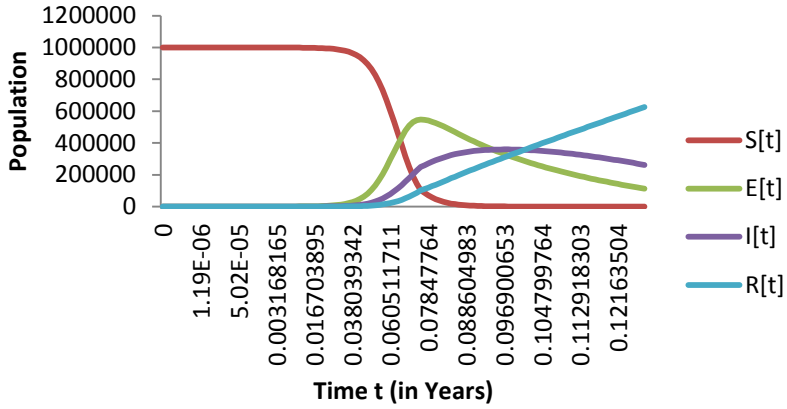

Figure 14.Using RUNGE-KUTTA method (α=0)

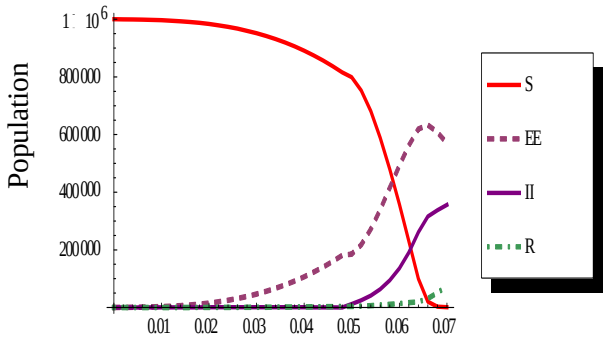

Time t (in years)

Figure 15.Using HAM (α=0.5)

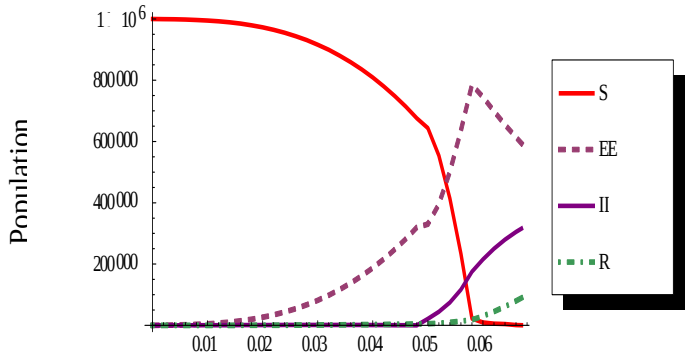

Time t (in years)

Figure 16. UsingHAM (α=1)

Variation of population with time for rubella